



AN INTERFACIAL FRICTION CORRELATION FOR SHELL-SIDE VERTICAL TWO-PHASE CROSS-FLOW PAST HORIZONTAL IN-LINE AND STAGGERED TUBE BUNDLES

F. H. RAHMAN, J. G. GEBBIE and M. K. JENSEN†

Department of Mechanical Engineering, Aeronautical Engineering and Mechanics, Rensselaer Polytechnic Institute, Troy, NY 12180-3590, U.S.A.

(Received 5 April 1993; in revised form 1 March 1996)

Abstract—A correlation is presented for the interfacial friction factor between the gaseous and liquid phases in vertical two-phase flows past horizontal in-line and staggered tube bundles. The interfacial friction data were determined from pressure drop, void fraction, and mass flux data taken by Dowlati *et al.* (1990, 1992b) and Schrage *et al.* (1988). These data were correlated using two non-dimensional quantities: a Reynolds number based on the mixture density and relative velocity between the two phases, and the porosity of the tube bundle. These dependencies are explained in terms of the competing effects of viscosity and buoyancy and the influence of turbulence in the flow. The correlation is implemented in a numerical simulation of the recirculating shell-side flow encountered in kettle reboiler heat exchangers, the results of which are compared to the experimental observations of Cornwell *et al.* (1980). Copyright © 1996 Elsevier Science Ltd.

1. INTRODUCTION

Shell and tube heat exchangers are among the most widely used type of heat exchangers. Utilized as reboilers, feedwater heaters, steam generators, and evaporators, applications are found in the chemical process industry, the power generation industry, and the refrigeration and air-conditioning industries. Of all the research performed on shell-side flows, parallel flow past vertical tube bundles has been studied extensively while little progress has been made on cross-flow through horizontal tube bundles. Only recently have researchers considered the local flow conditions in the latter case when predicting the overall performance of the heat exchanger. Such an analysis is particularly important in kettle reboiler heat exchangers where variations in the operating conditions can have significant effects on the local flow conditions, which in turn will affect the overall performance. It is important to establish design correlations with which the local heat transfer and flow conditions can be predicted for such flows. This will facilitate an understanding of the effects of the various flow parameters and the operating conditions on the overall performance of the heat exchanger.

State-of-the-art predictions on the local flow conditions in shell-side flow rely on numerical solutions of the governing fluid flow and heat transfer equations. In considering the two-phase flow equations, the existence of a relative velocity between the phases requires the solution of the velocity field for each phase. In writing the conservation equations of each phase, the balance laws between the two phases are required for the closure of the equations. In the case of the momentum equation, this balance law comes in the form of an interfacial momentum transfer (or interfacial friction) constitutive law. While the basis of this law must rely on the micro-physics of the interaction between the two phases across their interface, it must also be provided as a function of the space and time-averaged flow conditions.

The interaction between the phases can be very complicated. The development of a constitutive law is a formidable task for researchers, especially since the connection between the micro-physics and the macro-flow conditions is difficult to establish. In light of the tremendous advances in numerical techniques and computing speeds, the predictive capabilities of a two-phase flow

† To whom any correspondence should be sent.

numerical model are limited by the accuracy and the generality of the interaction terms and, in particular, the interfacial friction correlation. This is in essence the distinguishing factor between numerical codes that predict two-phase flows through tubes and those that can predict the shell-side cross-flow past tubes. In the case of kettle reboilers, the interfacial friction correlation is particularly important since the flow across the tubes is caused by natural circulation. The buoyancy of the gaseous phase drives the circulation and affects all other flow conditions solely through the interfacial friction.

All past research that has been done on interfacial friction has been limited to in-tube flows. Yet, in spite of the relatively simple geometry, the success of these models has been limited to flows of low void fractions and those that exhibit a limited range of interfacial slip. Because shell-side flows are through much more complex geometries they are expected to display elevated levels of turbulence and may span several flow patterns; it would not be prudent to use in-tube correlations for such flows. The data that form the basis of the in-tube correlations do not include flows with similar characteristics as shell-side flows and, therefore, these correlations are not expected to remain accurate over the spectrum of bubble sizes, shapes, and distributions that may be encountered in shell-side flows.

In the past, as a consequence of the dearth of appropriate correlations, shell-side flow researchers have been forced to use in-tube correlations or the homogeneous flow assumption. The former method has proved to be restrictive in that it relies on trends that have no fundamental grounds and can only be used strictly within the range of the experimental data. Edwards & Jensen (1991) have shown that the relative velocity encountered on the shell side of kettle reboiler heat exchangers is much larger than those that can be computed using interfacial friction correlations that were developed for bubbly flow within tubes. Furthermore, they demonstrate that the flow conditions are greatly affected by the choice of interfacial friction correlations. They observed that a constant interfacial friction factor much lower than those found in in-tube flows is insufficient to accurately predict all the flow conditions.

For in-tube flows, Ishii & Zuber (1979) present several different interfacial friction correlations, each spanning different bubble size ranges. In their "undisturbed" bubble correlation, the dominant mechanisms for general multi-particle systems is assumed to be the same as that for a single particle flowing through an infinite continuous phase. The interfacial friction correlation for the multi-particle system is, therefore, of the same form as that established for the single particle case (i.e. $C_D = f(\text{Re})$). Adjustments due to the effects of the interaction between the particles is achieved by including a mixture viscosity in the non-dimensionalization; the viscosity of the continuous phase as seen by each individual bubble is affected by the higher concentration of bubbles in the flow. The mixture viscosity is, therefore, included in a Reynolds number which is based on the relative velocity between the two phases. The "dirty water" interfacial friction correlation established by Wallis (1976) is the same as the undisturbed bubble model of Ishii & Zuber (1979) except without the mixture viscosity and the Stokes drag term. Wallis uses slightly different coefficients in his correlation to accurately predict the data.

Ishii & Zuber (1979) also present the "distorted" bubble interfacial friction correlation by extending the same idea to flows with larger bubbles. In this correlation the steady drag on the bubbles depends on the balance of the buoyancy to the viscous forces and are greatly affected by the turbulence induced by the motion of the preceding bubbles. The form of the correlation is obtained by assuming that the ratio of the drag coefficient of multi-particle systems to single particle systems is the same in the distorted bubble regime as in the undisturbed particle regime.

In all the correlations discussed thus far, the diameter of a typical bubble in the flow is employed as the length scale for non-dimensionalization. The implementation of these interfacial friction correlations requires a flow pattern map to distinguish the flow regimes and a method of computing the bubble length scale used in the non-dimensionalization. This is seen in the interfacial drag correlation used in the RELAP code (Ardron & Clare 1989). The complicated flow pattern map is based on the void fraction and total mass flux of the flow. These schemes require the prediction of the bubble size as the length scale for non-dimensionalizations that are independent of any prescription given by the correlation. For a given flow condition, a range of bubble sizes may exist. The relationship between the physical bubble size and the

length scale employed in the correlation becomes unclear and introduces added uncertainty to the correlation especially when, in a numerical scheme, the length scale must be determined from observable flow conditions. In practice, the experimental determination of this length scale is extremely difficult and even harder to correlate.

Lahey *et al.* (1979) show that for bubbly flows the interfacial friction varies as a function of the radial location from the center of the tube. It is found to be a multi-valued function of the void fraction. They claim that the sophistication required to predict these trends is clearly beyond the present understanding of the phenomena and conclude that the state of the art remains a one-dimensional averaged correlation. They proceed by using a simple curve fit, with the drag variation linear with void fraction, to correlate the one-dimensional averaged interfacial friction at a single liquid mass flux. Other attempts at developing interfacial friction correlations have met with less acceptance. The Los Alamos Scientific Laboratory correlation (Amsden *et al.* 1979) analyzes the flow in terms of a conglomeration of hypothetical liquid and vapor "drops" each having a dominant length scale. The interfacial momentum transfer is then inferred through a heuristic argument based on the momentum transfer that would occur due to the collisions of these "drops". The final expression for the interfacial friction is found to be independent of the viscosity and is a linear function of the void fraction.

All of the preceding correlations are for in-tube flows. No interfacial friction correlations have been established for shell-side flows. The work presented here will develop an interfacial friction correlation for vertical shell-side flows past both in-line and staggered tube bundles. These flows are significantly different in character than in-tube flows and, therefore, the interfacial friction characteristics are expected to be different.

2. THE INTERFACIAL FRICTION DATA AND CORRELATION

The interfacial friction data used in the development of the correlation are obtained from the experimental results of Dowlati *et al.* (1990, 1992b) and Schrage *et al.* (1988).

Dowlati *et al.* performed a series of experiments on adiabatic (air/water at atmospheric pressure), vertical cross-flow past six different tube bundles. Two of the bundles had square in-line geometry, with the pitch-to-diameter ratios, P_1/D , of 1.30 and 1.75. Two bundles had rectangular in-line geometries with longitudinal pitch-to-diameter ratios of $P_1/D = 1.33$ and 2.17 (each had the same transverse pitch-to-diameter ratio of $P_1/D = 1.75$). The remaining two bundles were in a staggered arrangement (equilateral triangle) with pitch-to-diameter ratios of $P_1/D = 1.30$ and 1.75 as measured by the length of a side of the triangle. Tube diameter in the 1.30 pitch-to-diameter ratio bundles was 0.01905 m. Tube diameter in the remaining bundles was 0.01270 m. The pressure drop across a specified number of tubes within the tube bundle test-section was measured together with the void fraction profile in the direction of the flow. This was done for a range of measured phasic mass fluxes. Using a single-beam gamma densitometer, the average void fraction in the area between two adjacent tube rows in the transverse direction was measured. The void fraction profile through the test-section was found to be constant in the direction of the flow. Because the pressure drop was moderate and the experiment was conducted adiabatically, the flow was non-accelerating and, hence, the constant void fraction profile is expected. No transverse variations were measured in the flow and, therefore, the experiments were one-dimensional in nature.

Schrage's experiments took place in a similar type of test section (again, air/water at atmospheric pressure) with a square in-line arrangement. The pitch-to-diameter ratio was 1.30 and the tube diameter was 0.00794 m. The void fraction was determined using the quick-closing valve technique and, in light of Dowlati's results, the void profile is assumed vertically and horizontally constant (again, one-dimensional flow).

The one-dimensional nature of the experimental data restricts the interfacial friction coefficient to a one-dimensional form. In order to obtain the average interfacial friction from the data, the flow through the tube array is represented by the use of porosity. The porosity, ϕ , represents the blockage to the flow due to the presence of the tubes. It is defined as the ratio of volume

accessible to the flow per unit volume and can be computed directly from the pitch-to-diameter ratio:

$$\phi = 1 - \frac{\pi}{4} \left(\frac{D}{P_t} \right) \left(\frac{D}{P_l} \right) \quad [1]$$

where P_t and P_l are the transverse and longitudinal pitch (the horizontal and vertical distances between the centers of two adjacent tubes), respectively. This notion of porosity is consistent with the state-of-the-art numerical modeling of the tube bundle in the kettle reboiler (Edwards & Jensen 1991). By incorporating the porosity, the variations in the phasic velocity as it negotiates its way past the tubes is averaged to a constant as is the cross-sectional area of the flow channel, and the void fraction of the flow field becomes the averaged void fraction measured experimentally.

The interfacial drag on a single bubble moving through a medium is defined by:

$$C_D = \frac{F_{D_B}}{\frac{1}{2} \rho_m v_r^2 A_B} \quad [2]$$

where F_{D_B} is the drag force on the bubble, v_r is the relative velocity of the bubble, ρ_m is the two-phase mixture density of the medium, and A_B is the projected area of the bubble. A control volume approach to [2] results in replacing F_{D_B} with F_{D_G} , and A_B with A_G (drag force on and area of the gaseous phase in the control volume, respectively).

If M_G^i is the interfacial drag force on the gaseous phase in the control volume, and the volume is V , then:

$$F_{D_B} = M_G^i V. \quad [3]$$

For adiabatic non-accelerating flows the time averaged vapor cross-sectional area fraction and the volumetric average vapor fraction (hold-up void fraction) are equivalent. The data analyzed in this research qualify as adiabatic and non-accelerating, therefore:

$$\epsilon = \frac{V_G}{V} = \frac{A_G}{A} \quad [4]$$

with V_G representing the volume of gas in a given control volume and A_G represents the gaseous area on a control surface within the same control volume. (Note: by convention an unsubscripted ϵ indicates the void fraction of the vapor phase.)

Furthermore, the ratio of gaseous volume to gaseous area is:

$$\frac{V_G}{A_G} = \frac{\epsilon L P_t P_l \phi}{\epsilon L P_t \phi} \quad [5]$$

since the porosity represents both the effective volume and cross sectional flow area of the control volume. L is the length of the tubes in the test section (and is, therefore, the depth of the control volume).

Combining [3]–[5] results in [2] taking the form:

$$C_D = \frac{2M_G^i P_t}{\epsilon \rho_m v_r^2}. \quad [6]$$

To obtain an expression for the interfacial momentum term we turn to the momentum equation for the gaseous phase:

$$\epsilon \frac{\partial p}{\partial y} + \epsilon \rho_G g + M_G^w + M_G^i = 0. \quad [7]$$

Equation [7] may be solved for the interfacial momentum term in terms of quantities which are known from the data except M_G^w which represents the momentum transfer between the tube (and test section) walls and the gas.

Experiments performed by Leroux & Jensen (1992) indicate that, except under thermal conditions at or exceeding the inception of the critical heat flux condition, the tube walls remain well wetted and vapor flows even in staggered tube bundles undergo little or no contact with the tube walls. This is especially true at low vapor mass qualities. It is, therefore, reasonable to assume

that the wall momentum source term is zero for both the tube and test section walls. With this assumption, [7] yields:

$$M_G^i = \epsilon \left(\frac{\partial p}{\partial y} + \rho_G g \right). \quad [8]$$

The pressure gradient in [8] is obtained from the overall pressure drop in the test section divided by the vertical distance between pressure taps. Pressure taps were placed by both Schrage *et al.* and Dowlati *et al.* so as to preclude entrance or exit effects.

The relative velocity in [6] may be calculated by subtracting the individual phase velocities which are obtained from:

$$v_k = \frac{W_k}{\epsilon_k \rho_k \phi A_0} \quad [9]$$

where W_k , ϵ_k , and ρ_k are the mass flow rate, void fraction, and density (respectively) of phase k . A_0 is the transverse open area of the test section ($A_0 = LP_i$) and, as before, is multiplied by the porosity to give the effective flow area. With [8] and [9], all of the terms in [6] may now be computed from the data. Note that ρ_m is computed from $\rho_m = \epsilon \rho_G + (1 - \epsilon) \rho_L$.

In reviewing the open literature on interfacial friction correlations it was apparent that two non-dimensional parameters are of primary importance. As stated in the introduction, Lahey *et al.* (1979) found that at a single liquid mass flux the drag coefficient was well correlated by a simple linear curve fit with the void fraction as the independent variable. Ishii & Zuber (1979) correlated the drag coefficient using a Reynolds number based on continuous phase density, relative velocity, bubble diameter, and mixture viscosity (which, in turn, was dependent on void fraction). Ardron & Clare (1989) correlated interfacial drag in a similar manner to Ishii & Zuber (1979) except that the liquid viscosity is used (in place of the mixture viscosity) and the liquid void fraction is included in the Reynolds number. While it is true that other dimensionless groups have been used to correlate drag (e.g. the Froude number based on superficial mass velocity), those that use the void fraction and some type of Reynolds number have been most successful. Attempts were made during the course of this research to correlate the drag using many of these groups. By far, the most successful independent variable chosen was a Reynolds number defined by:

$$Re = \frac{\rho_m v_r \delta}{\mu_L} \quad [10]$$

where δ is computed as the porosity times the transverse pitch ($\delta = \phi P_i$). This provides a characteristic length (hydraulic diameter for porous media) that becomes more restrictive for "less porous" tube arrangements. This Re number contains the dependency on void fraction (ρ_m and v_r) as well as characterizing the flow by the liquid and vapor velocities (v_r).

A plot of the interfacial friction coefficient versus the Reynolds number is shown in figures 1 and 2 for in-line and staggered bundles, respectively. For a given porosity these data are clearly well characterized by a power law dependence on Re. Two regions of different slopes are evident in each plot. These regions are separated at $C_D \approx 4$ and will be referred to as the "upper region" ($C_D > 4$) and the "lower region" ($C_D < 4$). The drag coefficient was chosen as the demarcation criterion because the transition point in terms of C_D remains fairly constant for the various geometries while the transitional Re changes.

Although a flow pattern map was unavailable for these data the reason for this separation between the upper and lower regions of the plots is hypothesized to be due to a change in flow pattern. Manifestation of these flow patterns through the rate of drag coefficient decrease with increasing Reynolds number may be discussed more effectively by replacing the relative velocity by $v_r = v_L(S - 1)$, where S is the slip ratio defined by v_G/v_L . Thus, we see that the relative velocity may be altered in two ways: a change in liquid velocity or a change in slip. Regions of high liquid mass flow and moderate to high mixture densities produce high Reynolds numbers and are represented by the "lower" portions of figures 1 and 2. These conditions are consistent with bubbly and slug flows. Low liquid mass flows and mixture densities are consistent with churn and spray/annular type flows and produce the low Reynolds numbers which represent the "upper" portions of figures 1 and 2. The rate of decrease of the drag coefficient must be described in terms

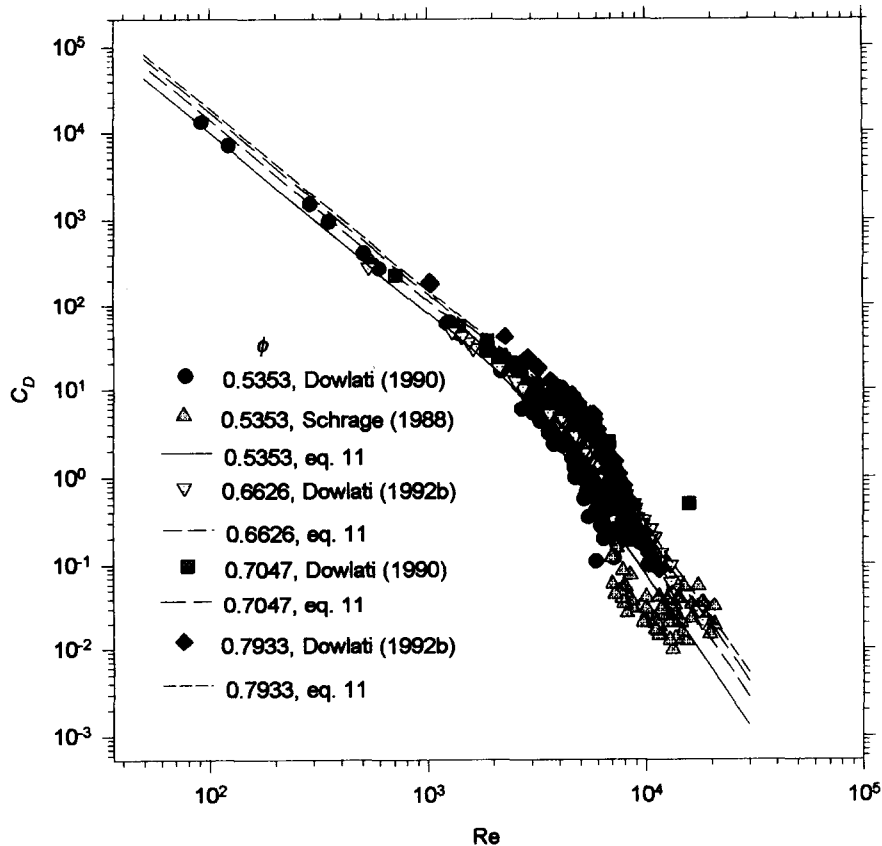


Figure 1. In-line tube bundle interfacial friction factor data and predictions by the correlation.

of the rates of increase in shear stress, slip, and buoyancy. In general, an increase in void fraction increases all of these factors. The shear stress term (numerator in [6]) increases less rapidly than the slip term (which is squared in the denominator) and the drag coefficient decreases. This behavior is found in both regions of the figures 1 and 2 and is consistent with the behavior of friction coefficients in single phase flows.

The explanation for the slope change between the two regions is found in the relationship between increases in shear and buoyancy. In churn flow, the flow is well mixed and the gaseous phase is dispersed. This dispersion increases the surface area to volume ratio which reduces the effect of buoyancy. The opposite behavior is found in bubbly and slug flows. The gaseous phase is less dispersed; in fact, bubbles tend to conglomerate and decrease the surface area to volume ratio and buoyancy becomes more dominant. Since buoyancy is found in the denominator of the drag coefficient, through the $\epsilon\rho_m$ term, the increased effects of buoyancy in bubbly and slug flow decreases the drag coefficient more rapidly than in churn flow.

The data of Schrage *et al.* (1988) which appear in the lower region of figure 1 show a great deal of scatter. Since these investigators utilized the quick closing valve technique to measure void fraction it is expected that these data will have more uncertainties than those of Dowlati. However, only data with uncertainties of less than 5% were utilized for the present research. A reasonable explanation for the additional variation could not be found. Although the Schrage in-line arrangement is of the same porosity ($\phi = 0.5353$) as Dowlati *et al.* (1990), the tube diameter used was much smaller (7.94 mm versus 19.1 mm). It is possible that there exists another flow pattern transition in this portion of the curve other than those discussed above. Inspection of the Schrage data in figure 1 reveals a similar trend to that of Dowlati for the same porosity at Reynolds numbers of about 9000, but the data tend to level out at the higher Reynolds numbers. The $\phi = 0.7933$ data of Dowlati show no such leveling trend (for similar Reynolds numbers) and simply continue down and mix with the Schrage data in a linear fashion.

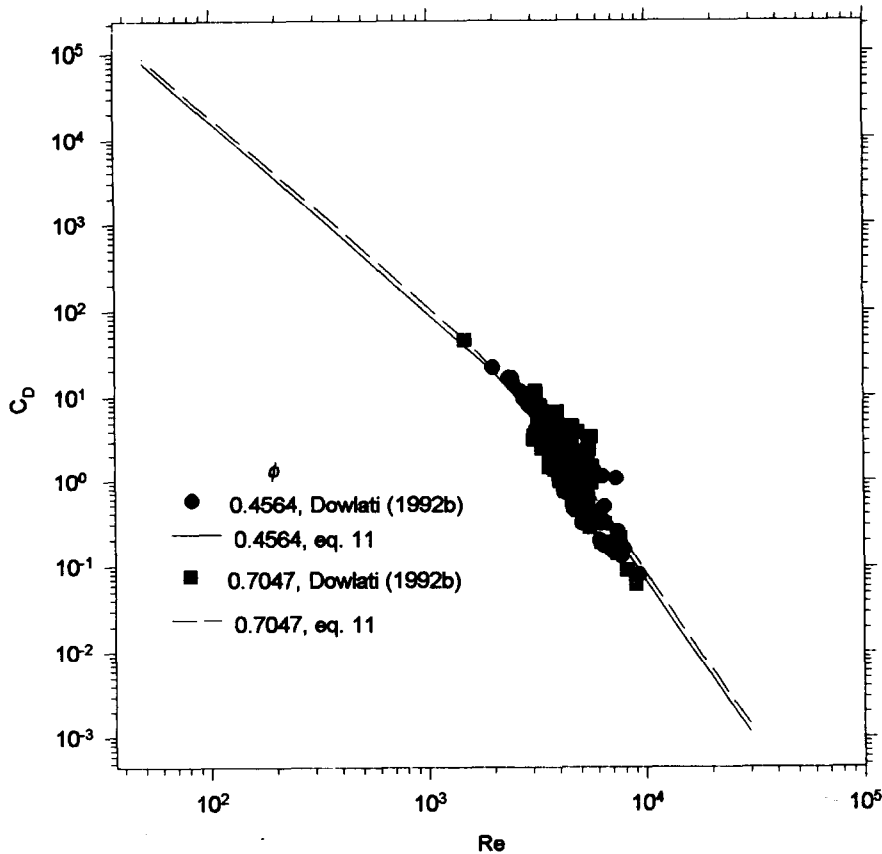


Figure 2. Staggered tube bundle interfacial friction factor data and predictions by the correlation.

Figure 1 shows that the interfacial friction coefficient is somewhat affected by the porosity with smaller porosities resulting in lower interfacial friction coefficients. This dependence is not captured by δ because, for the same porosity, δ may have different values depending on P_t . A completely satisfying explanation for this phenomenon was not found; however, a smaller porosity will encourage mixing, resulting in two effects. First, the bubbles will be more dispersed which will increase the surface area to volume ratio of the gaseous phase increasing the viscous drag relative to the buoyancy. Second, the increased mixing will tend to decrease the slip ratio between phases and, therefore, shear. The second effect seems to be somewhat larger than the first, thus resulting in smaller drag coefficients for the less porous test section. The effect of porosity is seen to be more pronounced in the lower portion of the curve than the upper. Porosity seems to have little effect on the drag in staggered bundles (figure 2).

3. RESULTS

The final correlation was obtained by arbitrarily demarcating the transition between the upper and lower regions by an interfacial friction coefficient of 4. The different regions were correlated using a simple power law dependence on the Reynolds number and the porosity. Chauvenet's criteria (Holman 1984) were used to eliminate four outlying data points from the upper and the lower correlations. The data were recorrelated without these data points. The upper and the lower correlations were then combined using the Churchill & Usagi (1972) expression. The final correlation is:

$$C_D = (C_{D_u}^{-4} + C_{D_l}^{-4})^{-0.25}. \quad [11]$$

The curve for in-line bundles was correlated separately from that of staggered bundles since different physics are suggested by the two types of geometry. With the porosity dependence assumed also to be captured by a power law, C_{D_u} and C_{D_l} each have the same basic form:

$$C_{D_{u \text{ or } l}} = e^E \varphi^\beta \text{Re}^\eta. \quad [12]$$

Values for the constants, E , β , and η are given in table 1 for each case. Although the same form was assumed for each type of geometry, the values for β in table 1 indicate that porosity has little effect on drag coefficient in staggered bundles. It should be pointed out that the staggered tube geometry is based on an equilateral triangle with sides equal to the transverse pitch; the longitudinal pitch is calculated as $P_1 = P_t \cos 30^\circ$. Ranges for porosity, void fraction, quality, and liquid mass flux from which the correlations were developed are:

for in-line bundles:

$$0.02 \leq \epsilon \leq 0.91$$

$$0.00 \leq x \leq 0.70$$

$$17 \leq G_L \leq 820 \text{ kg/m}^2\text{s}$$

$$92 \leq \text{Re} \leq 21,000$$

for staggered bundles:

$$0.03 \leq \epsilon \leq 0.90$$

$$0.00 \leq x \leq 0.15$$

$$56 \leq G_L \leq 800 \text{ kg/m}^2\text{s}$$

$$1500 \leq \text{Re} \leq 9300.$$

In spite of the arbitrary choice for the demarcation between the two regions, it should be noted that the correlation was in no way forced to transition at that particular location. In the final expression, the point of transition can be found approximately by equating the expression for the upper region with the expression for the lower region and solving for the Reynolds number.

Figures 1 and 2 show the curves that are predicted by the interfacial friction correlation. The porosity effects have been accurately correlated for the two types of geometry and, as noted early, porosity has a much smaller effect in staggered bundles. An evaluation of the predicted and actual values shows that the correlation produces a root mean square error of 51 and 47% for in-line and staggered bundles, respectively. As will be seen below, this variability is better than that required to produce good results in a numerical analysis of a tube bundle. Also, in light of the variation in geometry, quality, and mass flows, these results are considered good.

4. IMPLEMENTATION OF THE CORRELATION

While this paper's objective is to present an interfacial friction correlation, as mentioned earlier, a numerical solution of the local shell-side fluid flow conditions and heat transfer is required to accurately predict the overall performance of shell and tube heat exchangers. Hence, this section briefly describes a numerical simulation and one result of the simulation simply to illustrate the correlation's implementation. The kettle reboiler numerical model is described in detail by Edwards (1990), Edwards & Jensen (1991), and Rahman (1992). The interfacial friction correlation is crucial for the success of such simulations. It remains to insert this correlation into a numerical model that simulates such flows in order to compare the results with those obtained using previous correlations and with experimental observations. It is worth mentioning, for clarity, that this is a matter of using the subject correlation to compute the interfacial momentum term, for a particular flow field

Table 1. Values for constants in [12]

	E	β	η
Upper/in-line	19.91	1.63	-2.10
Lower/in-line	33.49	3.49	-3.68
Upper/staggered	20.17	0.31	-2.22
Lower/staggered	31.97	0.53	-3.72

using [7]. This will be an iterative process that can be summarized by (on a per control volume basis, and ignoring the energy equation for this example):

- (1) Calculate δ , ϕ , P_l , and P_t (geometric parameters).
- (2) Provide initial guesses for v_L , v_G , and ϵ .
- (3) Calculate ρ_m , v_r , and Re (the latter from [10]).
- (4) Calculate the drag coefficient from [12].
- (5) Calculate the interfacial momentum exchange term, M_G^i , by rearranging [6].
- (6) Use the interfacial momentum calculated in the basic momentum equations (e.g. [7]).
- (7) Check to see if the governing equations (mass, momentum) are satisfied.
- (8) If the governing equations are not satisfied, update the guesses in velocities and void fraction and proceed to step 3.

The two-fluid, two-dimensional finite difference numerical model in which the interfacial friction correlation is tested uses geometric parameters of a kettle reboiler that duplicate the test-section employed by the experiments of Cornwell *et al.* (1980). This model simulates the flow at a cross-section of the reboiler containing 241 tubes in a square in-line array with pitch-to-diameter ratio 1.33. The recirculating flow is driven by the rising vapor which is generated in the tube bundle. The vapor escapes to atmospheric conditions across a free surface at the top of the reboiler while the liquid recirculates back through the tube bundle. The replenishing liquid enters the heat exchanger from an inlet at the bottom center of the shell. The working fluid is refrigerant R113.

The flow characteristics within the reboiler are determined by solving the two-dimensional transient mass and momentum conservation equations simultaneously using a commercially available computer code entitled PHOENICS, which is capable of integrating several parabolic, hyperbolic, or elliptic partial differential equations simultaneously using the SIMPLEST algorithm and a staggered grid discretization. In order to reduce the complexity of the problem at hand to a tractable level, the flow is assumed to be a saturated liquid/vapor mixture with constant properties everywhere. Consequently, the temperature is uniform within the kettle reboiler, eliminating the need to solve the energy equation. Although only the steady state solution is sought, the transient equations are solved to facilitate numerical convergence.

To expedite the computation, a coarse discretization was employed (square cells of length equal to the tube pitch). The flow past the tube bundle is modeled using porosity as defined in the development of the interfacial friction correlation. Likewise, the circular shell of the reboiler was simulated using fully blocked cells, or zero porosity cells. The boundary conditions of the model were: no-slip, solid walls along the circular shell, a vertical line of symmetry through the center of the reboiler, one atmosphere outlet pressure at the top of the reboiler, and a saturated liquid flow rate through the inlet in the bottom of the reboiler. The outlet permitted only the passage of vapor, the flow rate of which was determined by the computed pressure field within the reboiler. The replenishing saturated liquid flow rate at the inlet was set to equal the flow rate of vapor leaving at the outlet. A constant wall heat flux at the tubes was used to model the electrically heated tubes used by Cornwell *et al.* (1980).

For closure of the governing fluid flow equations, the wall friction correlation presented by Schrage *et al.* (1988) was used together with two different interfacial friction correlations. The results using two different interfacial friction correlations are presented and qualitatively compared with the experimental results of Cornwell *et al.* (1980). A constant interfacial friction setting, previously used by Edwards & Jensen (1991), is employed for comparison. According to Edwards & Jensen (1991), this interfacial friction setting produced results which were superior to those obtained using correlations developed from in-tube flow data. This alternate interfacial friction coefficient, C_{fps} , is the default setting in PHOENICS and is defined by:

$$M_G^i = C_{fps} \epsilon (1 - \epsilon) \rho_L \quad [13]$$

Edwards & Jensen (1991) used a constant of 10.0 for this interfacial friction coefficient throughout the kettle reboiler domain. For further details on correlation implementation using PHOENICS and convergence criterion the reader is referred to Edwards (1990) as well as Rahman (1992).

The results from the numerical model are presented as void fraction contour plots and vector plots of the total mass flux based on the free cell area. The results using the constant interfacial

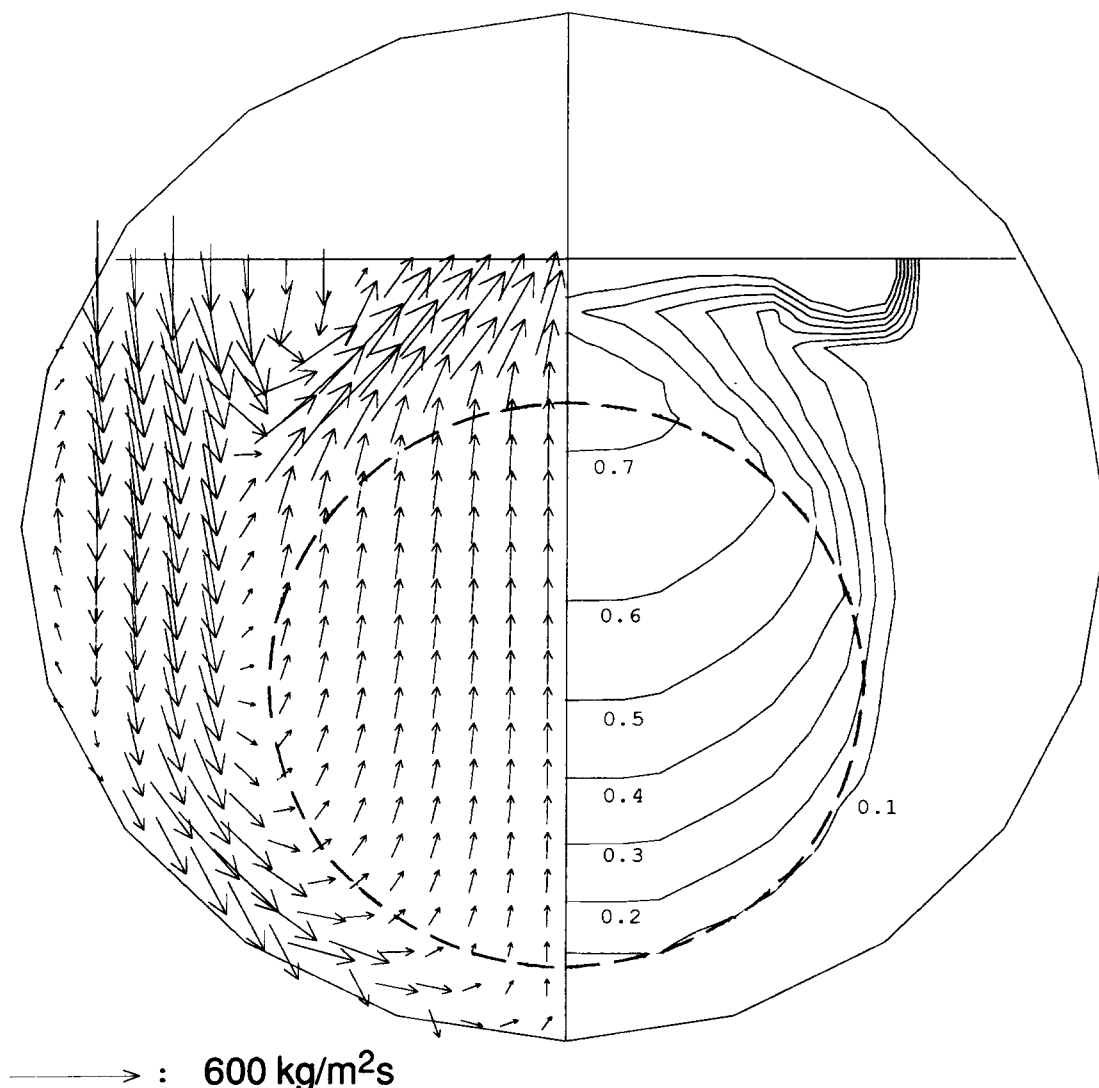


Figure 3. Void fraction contour plot and total mass flux (based on the free cell area) vector plot obtained at a constant wall heat flux of 20 kW/m^2 using the constant interfacial friction setting with $C_{f,ps} = 10$.

friction setting and the new interfacial friction correlation are given in figures 3 and 4, respectively. In these figures the dotted circle represents the outer boundary of the tube bundle.

While the general flow patterns displayed in figures 3 and 4 are similar, several significant differences can immediately be noted, particularly with the flow inside the tube bundle. Unlike the constant interfacial friction setting, the void fraction results obtained by using the interfacial friction correlation separate two distinct regions in the tube bundle by a narrow band over which the void fraction increases from 0.1 to 0.7. The numerical model using the correlation shows that the slip ratio in the lower voidage area is significantly higher (ranging from 47 to 60) than in the high voidage area, where the flow approaches homogeneous flow. The vector plot of figure 4 also distinguishes these two regions of the tube bundle: in the higher voidage region the flow is vertically upwards and of large magnitude, whereas in the low voidage region the flow has significant horizontal components and is of smaller magnitude. Lastly, figure 4 shows much of the flow in the bundle to be skewed toward centerline from vertical. This indicates that much of the flow enters the bundle along two-thirds of the perimeter rather than being limited to the lowest portions as is the case in figure 3.

Figure 5 shows a contour plot of the interfacial friction factor, obtained using the correlation presented here, within the modeled heat exchanger. Overall the friction factor is seen to vary by

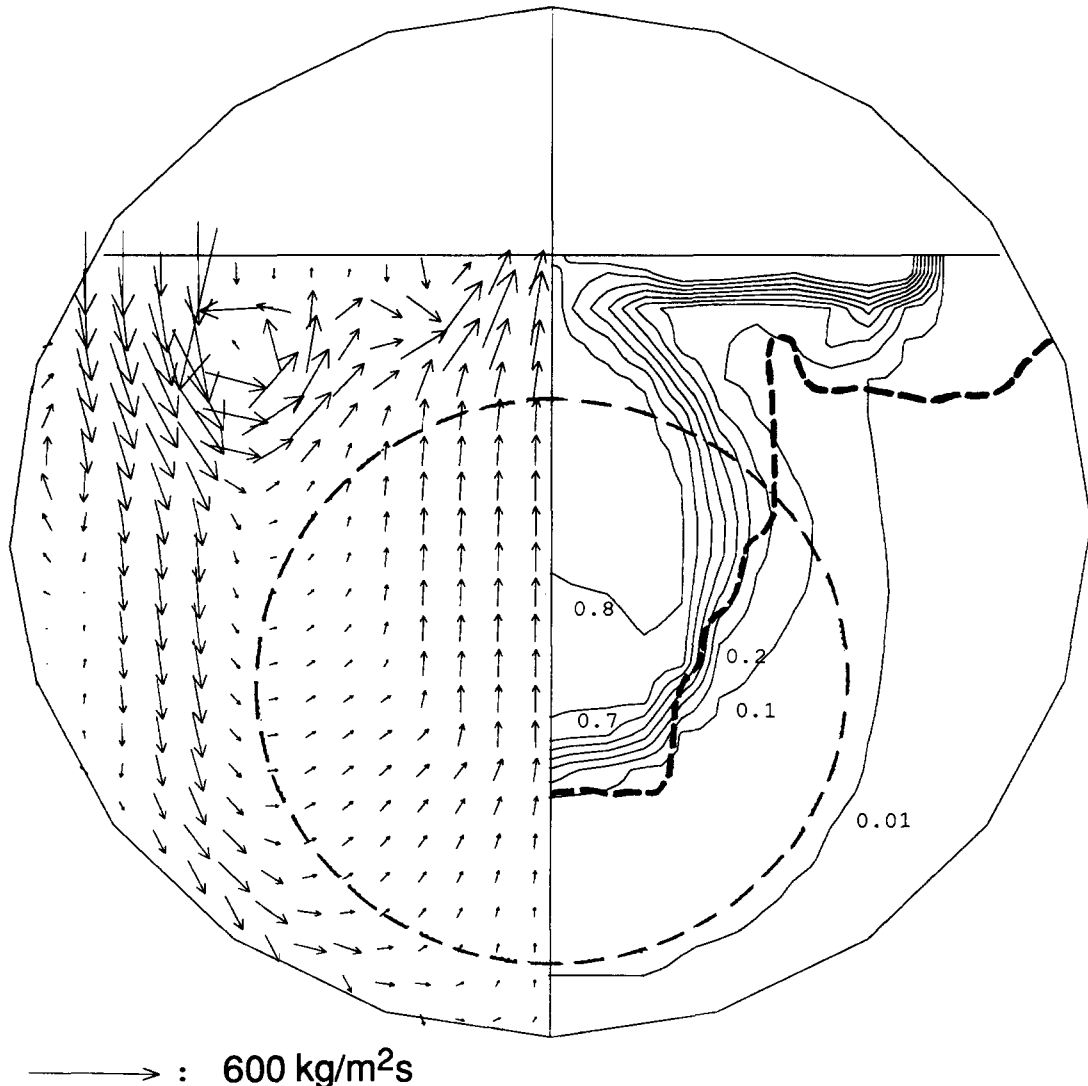


Figure 4. Void fraction contour plot and total mass flux (based on the free cell area) vector plot obtained at a constant wall heat flux of 20 kW/m^2 using the interfacial friction correlation. Heavy dashed line indicates dividing line between high void and low void regions from data of Cornwell *et al.* (1988).

more than six orders of magnitude and by four orders of magnitude in the region of most rapid void fraction increase. Clearly, the $\approx 50\%$ (RMS error) variation of drag coefficient found in the correlation is insignificant. Flow pattern observations of kettle reboilers by Gebbie (1994) and King (1992) indicate these high and low void fraction regions are frothy/churn and bubbly/slug flows, respectively, which justifies the above explanation for the drag coefficient variations in different flow regimes.

The dashed line in figure 4 represents the lower boundary of the “high voidage” region as determined from visual observations by Cornwell *et al.* (1980). In this region Cornwell describes the flow to be a frothy, two-phase mixture with high speeds. The flow in the area between adjacent tube columns was noted to consist predominantly of liquid. Cornwell *et al.* (1980) state that the boundary between the two regions to be distinct, implying a quick transition to the frothy flow pattern. In the low voidage region the flow was observed to be bubbly to the extent that it “differed little from single phase flows”. A comparison of the boundary between the high and low voidage regions predicted using the new interfacial friction correlation and the observations of Cornwell *et al.* (1980) shows a remarkable resemblance which does not exist if the constant interfacial friction setting is used. Furthermore, the flow directions in the two regions of the bundle are identical to those described by Cornwell *et al.* (1980).

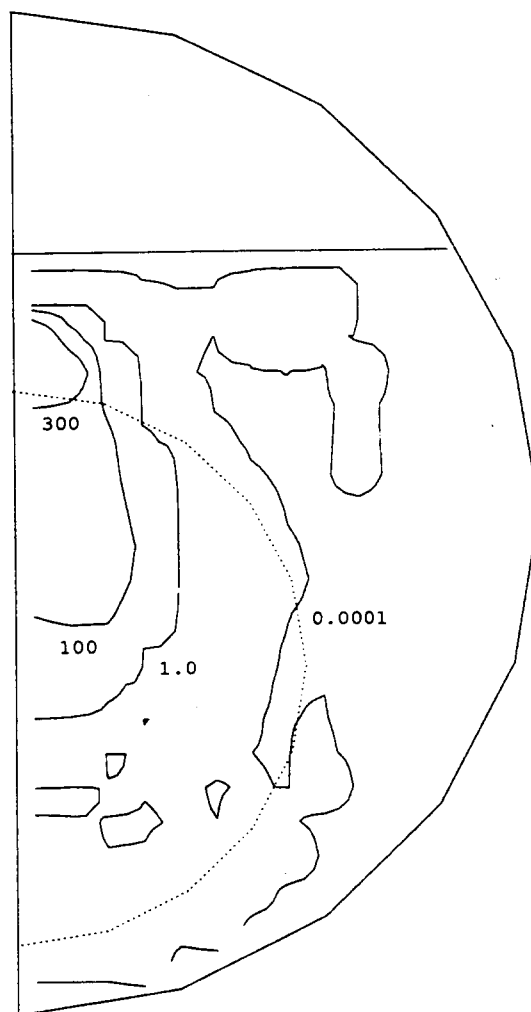


Figure 5. Drag coefficient contour plot at a constant wall heat flux of 20 kW/m^2 using the interfacial friction correlation.

As yet the comparison to experimental studies on cross-flow through tube bundles are largely restricted to qualitative observations. Due to the immense difficulties in accurately measuring the local void fractions and phasic velocities within the tube bundle, limited void fraction data and no phasic velocity data are presently available. The quantitative predictions of the numerical model, therefore, have not been verified.

The results of the numerical model have demonstrated the necessity of an appropriate interfacial friction correlation for shell-side flow and have displayed the vast improvement in predictive capabilities which follow from it. The flow pattern transition suggested by the computed void fraction profile follow directly from the extreme interfacial friction gradients in the tube bundle domain. While such variations cannot be accommodated by either a constant, low interfacial friction setting or correlations developed for in-tube flows, such variations also imply that the model is insensitive to the relatively small uncertainties of the interfacial friction correlation. The important feature of the correlation is its ability to predict the large gradients.

5. CONCLUSIONS

Interfacial friction correlations have been developed for vertical shell-side flow past horizontal, in-line and staggered tube bundles. The correlations are expected to be valid for bubbly, slug, and churn-turbulent flow patterns, but not necessarily for spray flows. The interfacial friction

experienced by these flows is observed to accommodate a much wider range of values compared to correlations for in-tube flows. This is seen by the wide range of slip ratios (from 1 to 60) which it allows.

A kettle reboiler numerical model using the newly developed interfacial friction correlation predicts all the qualitative features of the flow within the tube bundle that have been observed experimentally. The enhanced predictive capability of this numerical model relies on the large variations in the interfacial friction within the solution domain. The large interfacial friction gradients which are noted in the tube bundle make the results from the numerical model insensitive to the relatively small uncertainties of the interfacial friction correlation. Such results cannot be predicted using correlations developed for in-tube flows.

6. NOMENCLATURE

A	Area (m^2)
A_0	Open channel cross-sectional area (m^2)
β	Parameter for [12] correlation
C_D	Interfacial friction coefficient defined by [6]
C_{fips}	Interfacial friction coefficient defined by [13]
δ	Tube bundle characteristic length (m)
D	Diameter of tube (m)
e	Base of the natural logarithm
η	Parameter for [12] correlation
E	Parameter for [12] correlation
ϵ_k	Void fraction of phase k (unsubscripted represents vapor void fraction)
g	Gravitational acceleration (m/s^2)
k	Subscript that can be L, G, or m (meaning liquid, gas, and mixture, respectively)
μ_L	Dynamic viscosity of liquid phase (kg/ms)
M_k^i	Volumetric momentum source term due to interfacial friction on phase k (N/m^3)
M_k^w	Volumetric momentum source term due to friction from the walls on phase k (N/m^3)
ϕ	Porosity, used to model flow past the tubes
p	Pressure shared by both phases (Pa)
P_t	Transverse pitch, the horizontal distance between adjacent tube centers (m)
P_l	Longitudinal pitch, the vertical distance between adjacent rows (m)
ρ_k	Mass density of phase k (kg/m^3)
Re	Reynolds number defined by [10]
v_k	Velocity of phase k (m/s)
v_r	Relative velocity, $v_G - v_L$ (m/s)
V	Volume (m^3)
W_k	Total mass flow rate of phase k (kg/s)
x	Vapor mass quality of the flow
y	Distance measured along the vertical direction (m).

Acknowledgements—This study was partially supported by the National Science Foundation (grant number CTS-9008435) and the Department of Mechanical Engineering, Aeronautical Engineering, and Mechanics at Rensselaer Polytechnic Institute. This assistance is gratefully acknowledged. We are grateful to Dr Dowlati, Mr Schrage, and their coworkers for sharing their experimental data without which this study could not have been accomplished. Appreciation to Dr Kawaji is extended for sending data to us.

REFERENCES

- Amsden, A. A., Butler, I. D. & Harlow, F. H. 1977 Numerical study of downcomer flow dynamics, July–December 1976, Los Alamos Scientific Laboratory Report LA-NUREG-6797-SR.
- Ardron, K. H. & Clare, A. J. 1989 Assessment of interphase drag correlations in the RELAP5/MOD2 and TRAC-PF1/MOD2 Codes, Report NUREG/IA-0015.

- Churchill, S. W. & Usagi, R. 1984 A general expression for the correlation of rates of transfer and other phenomena. *AIChE J.* **18**, 1121–1128.
- Cornwell, K., Duffin, N. W. & Schuller, R. B. 1980 An experimental study of the effects of fluid flow on boiling within a kettle reboiler tube bundle, ASME Paper No. 80-HT-45.
- Dowlati, R., Chan, A. M. C. & Kawaji, M. 1992b Hydrodynamics of two-phase flow across horizontal in-line and staggered rod bundles. *J. Fluids Engineering* **114**, 450–456.
- Dowlati, R., Kawaji, M. & Chan, A. M. C. 1990 Pitch-to-diameter effect on two-phase flow across an in-line tube bundle. *AIChE J.* **36**, 765–772.
- Dowlati, R., Kawaji, M. & Chan, A. M. C. 1988 *Void Fraction and Frictional Pressure Drop in Two-phase Flow Across a Horizontal Tube Bundle*, AIChE Symposium Series No. 263, pp. 126–132.
- Edwards, D. P. & Jensen, M. K. 1991 A two-dimensional numerical model of two-phase heat transfer and fluid flow in a kettle reboiler. In *Phase Change Heat Transfer—1991* (Edited by Hensel, E., Dhir, V. K., Greif, R. & Fillo, J.), ASME, New York, HTD Vol. 159, pp. 9–16.
- Edwards, D.P. 1990 A two-dimensional numerical model of two-phase heat transfer and fluid flow in a kettle reboiler, M.Sc. Thesis, Rensselaer Polytechnic Institute, Troy, New York.
- Gebbie, J. G. 1994 Void distribution measurements in a kettle reboiler and submerged evaporator, M.Sc. Thesis, Rensselaer Polytechnic Institute, Troy, New York.
- Grant, I. D. R. & Chisholm, D. 1980 Horizontal two-phase flow across tube banks. *Int. J. Heat and Fluid Flow* **2**, 97–100.
- Holman, J. P. 1984 *Experimental Methods for Engineers*, Fourth Edition, Chapter 3. McGraw-Hill Book Co., New York.
- Ishii, M. & Zuber, M. 1979 Drag coefficient and relative velocity in bubbly, droplet or particulate flows. *AIChE J.* **25**, 843–855.
- Jensen, M. K. 1988 Boiling on the shellside of horizontal tube bundles. In *Two-phase Heat Exchangers; Thermal-Hydraulic Fundamentals and Design* (Edited by Kakac, S., Bergles, A. E. & Fernandes, E. O.). Kluwer Academic Publishers, New York.
- King, M.P. 1992 An experimental investigation of the local heat transfer distribution and flow patterns in kettle reboilers and submerged evaporators, M.Sc. Thesis, Rensselaer Polytechnic Institute, Troy, New York.
- Lahey, R. T., Sim, S. & Drew, D. A. 1979 An evaluation of interfacial friction drag models for bubbly two-phase flows. In *Nonequilibrium Interfacial Transport Process*, ASME, New York, pp. 11–17.
- Leroux, K. M. & Jensen, M. K. 1992 Critical heat flux in shellside boiling on horizontal tube bundles in vertical crossflow. *J. Heat Transfer* **114**, 179–184.
- Rahman, F. H. 1992 An interfacial friction correlation for vertical two-phase cross-flow through horizontal tube bundles and its implementation, M.Sc. Thesis, Rensselaer Polytechnic Institute, Troy, New York.
- Schrage, D. S., Hsu, J. T. & Jensen, M. K. 1988 Two-phase pressure drop in vertical crossflow across a horizontal tube bundle. *AIChE J.* **34**, 107–115.
- Wallis, G. B. 1976 Separated slow model of two-phase flow, Report No. ERPI NP-275.